https://doi.org/10.1016/j.supflu.2020.105046

Model assisted supercritical fluid extraction and fractionation of added-value products from tobacco scrap

Gerardo Joaquín Tita[a], Alexander Navarrete[b], Ángel Martín[c], María José Cocero[c*]

[a] Grupo Interdisciplinario en Materiales-IESIING, Facultad de Ingeniería, Universidad Católica de Salta, INTECIN UBA-CONICET, Campo Castañares s/n, Salta (A4402FYP), Argentina.

[b] Institute for Micro Process Engineering (IMVT), Karlsruhe Institute of Technology, Hermann-von-Helmholtz-Platz 1, 76344, Eggenstein-Leopoldshafen, Germany

[c] BioEcoUva, Research Institute on Bioeconomy. High Pressure Processes Group. Department of Chemical Engineering and Environmental Technology, University of Valladolid, c/ Doctor Mergelina s/n 47011 Valladolid (Spain)

[*]Corresponding author: Alexander Navarrete

Abstract

Residues of the tobacco industry are a source of valuable compounds such as solanesol and nicotine. In this work, the supercritical fluid extraction of these compounds from tobacco scrap was studied. The effect of the key process parameters (pressure, temperature, extraction time) was analyzed and a phenomenological model of the extraction was applied in order to derive solubility and mass transfer coefficients. Furthermore, solanesol and nicotine obtained by supercritical extraction were fractionated by means of a liquid-liquid extraction. Results show that different conditions are required depending on the purpose of the extraction: low pressure (15 MPa) in order to enhance solanesol yield and solanesol selectivity, and high pressure (37 MPa) to promote nicotine extraction, while model results indicate that the best results were obtained in conditions in which the extraction was controlled by the solubility parameters. These results provide indications for the valorization of residues produced by the tobacco industry.

https://doi.org/10.1016/j.supflu.2020.105046

1. Introduction

In 2018, 8,3 million tons of tobacco were produced worldwide. China produced 53,8% of this amount, followed by Brazil (9.1%), India (9%), USA (2,9%), Indonesia (2,2%), Zimbabwe (1,6%), Zambia (1.4%) and Argentina (1.3%) [1]. In Argentina, 63% of the production in 2017 corresponded to the Virginia variety, amounting about 73 million kilograms, produced mostly in the Salta and Jujuy provinces. In these provinces, the income of 82 000 persons depended on the tobacco industry in 2010 [2].

Tobacco leaves are classified according to their position in the stem as top, middle and bottom leaves. Top leaves are generally considered as the best fraction and their quality is associated to a high content of sugar and nicotine and a low content of other nitrogen compounds [3]. Plant stems are not used by the tobacco industry and they are usually employed in farms for soil conditioning [4], and the processing of leaves produces scrap as a second waste fraction.

Tobacco has several advantages as a raw material for a biorefinery. Tobacco cultivations show high biomass yields and tobacco plants have low lignin contents compared to typical forest biomass. Moreover, the tobacco industry produces a big fraction of waste, which represents about 30-35% of the total amount of biomass introduced to the process (i.e. excluding plant stems). This fraction contains a wide range of added-value compounds such as easily extractable free sugars [5], squalene [6], food-grade proteins [7] and bioactive compounds such as solanesol [8] and nicotine [9].

Solanesol ($C_{45}H_{74}O$, MW: 631.086 g/mol) is a terpene alcohol constituted by nine isoprenoid units. Solanesol is present in the leaves of solanaceous plants such as potato (in concentrations ranging from 0.04% to 0.4%), eggplant (0.2-0.4%), pepper (0.35-0.9%) and tomato (0.1-0.35%), but tobacco leaves show the highest contents of solanesol, which in the case of Virginia tobacco is (in dry basis): 5.7%-6.4% in leaves and 0.6%-1.9% in stems [10, 11]. Solanesol and the derived esters are bioactive with antibacterial, antiviral, antifungal, antiinflammatory and antiulcer

https://doi.org/10.1016/j.supflu.2020.105046

properties, among others [10]. The main use of solanesol in the chemical and pharmaceutical industry is as precursor in the chemical synthesis of Coenzyme Q10 and vitamin K analogues [12,13,14], and in the biological synthesis of Coenzyme Q10 using *Rhodobacter sphaeroides* [15], *Rhodospirillum rubrum* [16] or *Sphingomonas spp*. [17]. Owing to these applications, Taylor et al. [18] foresee an increased commercial value of solanesol.

On the other hand, nicotine ($C_{10}H_{14}N_2$, MW: 162.263 g/mol) is an alkaloid that is well known for its presence in tobacco and, more recently, in electronic cigarettes, and for the negative effect of these products on health. In addition, it has pharmaceutical applications as stimulant, active principle in products for the treatment of tobacco use disorders and also in pharmaceutical products for the treatment of Alzheimer's [26] and Parkinson's diseases [27]. Due to these applications nicotine has a considerable commercial value.

Usually, solanesol is extracted using organic solvents such as ethanol, hexane, methanol and ether [19]. However, these methods have well-known drawbacks related to the use of toxic solvents which must be removed from the final product, increasing costs. In contrast, supercritical CO_2 extraction presents obvious advantages as CO_2 is a non-toxic solvent that can be easily removed from the final product by depressurization, and as outlined in Table 1 several previous studies have demonstrated the feasibility of CO_2 extraction of solanesol from tobacco plants, yielding extracts with up to 20-30% of solanesol content. For example, Ruiz Rodriguez et al. [20] studied the supercritical CO_2 extraction of solanesol from tobacco, considering also the simultaneous extraction of nicotine. They obtained a maximum ratio of 18.91 g solanesol/g nicotine operating at 8 MPa and 25 °C (CO_2 density: 778 kg/m^3). With respect to the total content of solanesol, the best conditions were 25 MPa and 50 °C obtaining 0.294 g solanesol/g extract (6 g solanesol/g nicotine). Wang et al. [21] pretreated the tobacco leaves with an extraction using a mixture of ethanol and hexane (4:6), which allowed increasing the solanesol content from 0.1 g solanesol/g extract to 0.44 g solanesol/g extract during the supercritical extraction. Moreover, they analyzed the effect of particle size, considering sizes of 175, 225 and 550 μm,

https://doi.org/10.1016/j.supflu.2020.105046

and observing a detrimental effect due to increased particle size on mass transfer and extraction yield. On the other hand, this pretreatment hinders the industrial application and the scale-up due to the use of a mixture of toxic organic solvents at a temperature near its boiling point (40-60 °C). Rincón et al. [22] studied the supercritical extraction of nicotine from tobacco waste (scrap and powder), with particles sizes ranging from 200 to 1000 μm. The best conditions were 30 MPa and 60 °C (CO_2 density: 830 kg/m^3), reaching a nicotine recovery ranging from 24% to 43%.

The aim of this work is to recover the high value-added fraction of solanesol from the scrap residue by means of supercritical CO_2 extraction. A post-extraction (liquid-liquid) at ambient conditions is performed to obtain the final product. The influence of the key process parameters is analyzed, and a mathematical model is developed to assist in the optimization of the process. The final purpose is to contribute to the valorization of waste and by-products of the Virginia tobacco industry.

Table 1: Supercritical CO_2 extraction of tobacco plant and tobacco plant residues: selected previous works

Raw material	Amount	Particle size	CO_2 density	P,T.	Flowrate	Solanesol Yield	Nicotine Yield	Extract Yield	Scale	Ref.
Leaves	14 cm^3	425 μm	605-880 (kg/m3)	8- 25 MPa 25 - 60 °C	3,5 g/min	0,104-0,294 (mg/mg extract)	0,012-0,049 (mg/mg extract)	s.d.	Lab.	[20]
Scrap	7 g	150-200 μm 200-300 μm 300-800 μm	222-910 (kg/m3)	10- 30 MPa 40 - 80 °C	1-2 LPM	0,045-0,125 (mg/mg extract)	-	7-48.8 (g/kg Raw Mat.)	Lab.	[21]
Scrap + powder (Leave residues)	100 g	200-1000 μm	500-900 (kg/m3)	15- 30 MPa 40 - 70 °C	0,1-1 LPM	-	0,0039 (mg/mg extract)	s.d.	Lab.	[22]
Scrap	600 g	500 μm	781-940 (kg/m3)	15- 37 MPa 40 - 58 °C	120-310 g/min	0,205-0,230 (mg/mg extract)	0,029-0,044 (mg/mg extract)	34.5-99.4 (g/kg Raw Mat.)	Pilot	This work

2. Materials and methods

2.1 Raw material and chemical compounds

https://doi.org/10.1016/j.supflu.2020.105046

For the $scCO_2$ extraction experiments, tobacco scrap, a by-product of the Virginia tobacco leaf de-stemming process, was used. Scrap is constituted by pieces of tobacco sheet smaller than 25 mm. This material was kindly provided by the Cooperativa de Productores Tabacaleros de la Provincia de Salta (COPROTAB).

The scrap was ground in a Retsch SM100 knife mill which has an integrated sieve to obtain an average particle size of 500 µm. The Solanesol (> 90% HPLC) and Nicotine (99% GC) standards were provided by Sigma-Aldrich. The liquid CO_2 was provided by Carburos Metálicos. The solvents used were analytical grade, n-Hexane (95%), ether (60 -80 °C) and absolute ethanol.

2.2 Supercritical CO_2 extraction

The supercritical extraction was carried out in a pilot plant with CO_2 recirculation whose scheme can be seen in Figure 1. The pilot plant has a 5 L extractor, a GO back pressure regulating valve (BP-66), a Dosapro diaphragm pump (MB 140 SL-10) that delivers a maximum pressure of 40 MPa and a maximum flow rate of up to 15 kg.h-1, and a separator where the extract is collected. The CO_2 mass flow is measured with a REHONIK (RHM-03) Coriolis type flowmeter.

The plant material is loaded into a basket with an internal diameter of 100 mm and 486 mm long inside the extractor. The extractor is closed with a conical lid using a hydraulic system that provides enough pressure to avoid CO_2 leaks. Once the extractor is sealed, the system is pressurized from the pump to the extractor with liquid CO_2 from a battery of pipes. Once the system has been filled with liquid CO_2, the extractor is pressurized with the pump and at the same time heated to the extraction temperature. This heating is done in a first stage with electrical resistances that surround the pipe from the pump to the extractor, and in a second stage the body of the extractor is also heated with electrical resistances. The pressure in the extractor rises from the pressure at which the liquid CO_2 enters to the extraction pressure. When the desired pressure value is reached the regulating valve is opened. This causes a drop in the pressure of the solvent, transforming it into a gaseous phase. Thus, when it enters the separator, the extract precipitates due to the low density of the gaseous CO_2. The separator has a spherical

https://doi.org/10.1016/j.supflu.2020.105046

valve at the bottom that allows the recovery of the extract as the extraction is being done, and in this way the extraction curves can be determined. The gaseous CO_2 leaves the separator at a pressure of about 6 MPa and enters a condenser that allows it to be liquefied by lowering its temperature, allowing the system to work in a closed circuit.

In the preliminary tests it was observed that after 3 hours of extraction 95% of the extract was recovered and to extract the remaining 5% it was necessary to employ 3 additional hours. For this reason, the time of extraction of the tests was fixed in 3 hours. Experiments were carried out with 300 g and 600 g of raw material, with a normal bed density (200 kg/m^3) and with a high bed density (280 kg/m^3) which was achieved by compacting it manually.

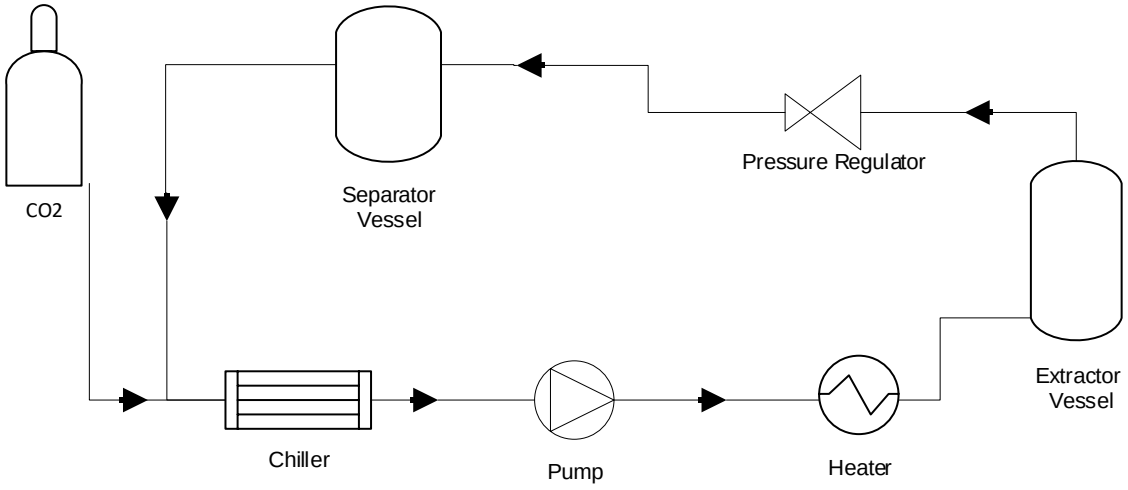

Figure 1: Schematic diagram of the supercritical CO_2 extraction plant

2.3 Liquid-liquid solvent extraction and fractionation

The liquid-liquid extraction was carried out on the basis of the method proposed by Hu et al. [23]. In this work, the extract obtained with scCO2 is subjected to a liquid-liquid extraction with petroleum ether and ethanol to separate the solanesol from the nicotine. This procedure differs from Hu, which performs a solid-liquid extraction of the tobacco residue with different proportions of petroleum ether and ethanol and then elutes the solution on a chromatographic column.

https://doi.org/10.1016/j.supflu.2020.105046

The liquid-liquid extraction consisted in dissolving 10 g of the extract in 300 mL of ethanol (adjusted to pH 2 with 1 mol HCl) at 32 °C for 3 hours in a magnetic stirrer. Then 200 mL of petroleum ether was added and continued to be shaken for 3 more hours. It was then placed in a separating funnel. The extract was kept homogeneous until 1 % v/v water was added and it was immediately separated into two phases.

The ethanol-water phase was washed 3 times with 50 mL of ether by gentle agitation in a separating funnel and finally all the ethanol was evaporated (with vacuum at 60 °C) in a rotary evaporator. To the residue of the rotavapor water with pH 10 was added to remove the nicotine. The water was removed, and the remaining residue was dissolved with petroleum ether and this solution was added to the ether phase of the first part of the liquid-liquid extraction.

The procedure used in this work seeks to separate nicotine from solanesol in the extract. Hu et al. [23] showed that in the first step of the liquid-liquid separation practically all the nicotine (98%) is transferred to the ethanol-water phase when it is acidified (pH=2) and practically all the solanesol (96%) is extracted in the organic phase when the pH of the aqueous phase is at the same value.

2.4 Product characterization

Residual humidity was determined measuring the weight reduction of 5 g of sample after 3 h of drying at 99.5^{o}C.

Nicotine concentration in samples obtained by supercritical fluid extraction was measured by Gas Chromatography with a flame ionization detector (GC/FID 7890A/G1888A Agilent), using a HP-5 column (length: 30 m, inner diameter: 32 mm, film thickness: 25 mm) and helium as carrier gas at a flowrate of 20 mL/min. Injector temperature was 300°C. A temperature ramp was used in the oven as follows: 50°C to 130°C at 5°C/min, 130°C to 250°C at 20°C/min, constant temperature at 250°C during 20 min, and 250°C to 300°C at 10°C/min.

https://doi.org/10.1016/j.supflu.2020.105046

A HPLC/DAD Alliance 2695 Waters with UV detector and a Symmetry C18 column (Waters, Particle size: 5 μm, Column internal diameter: 4.6 mm, column length: 150 mm) was used for qualitative and quantitative analyzes of solanesol and nicotine.

Solanesol concentration both in samples obtained by supercritical extraction and solvent extraction was determined using a mobile phase composed by acetonitrile:2-propanol (60:40 v/v) mixture at 1 mL/min, and a UV detector set at a wavelength of 210 nm.

Nicotine concentration obtained in liquid-liquid extraction was analyzed using a mobile phase of methanol:aqueous solution of 0.2% triethylamine (4:6,v/v) at a flow rate of 0.8 mL/min and detected at 254 nm. All samples were filtered through 0.45 μm membrane filter before injection.

2.5 Phenomenological model of the supercritical fluid extraction

The mathematical model developed by Cabeza et al. [24] was used to model the extraction curves obtained during our experiments. This model is based on the description of the extraction process presented by Sovová et al. [25] that considers three stages of separation. The first stage of extraction is controlled by external transport, the second stage is controlled by both external transport and internal diffusion, and the third stage is controlled by internal diffusion. Based on this description, Cabeza et al. [24] defined a global mass transfer coefficient, presented in equation 1. In this equation, $k_{SCF}.a_{SCF}$ characterizes the mass transfer during the stage of external mass transfer, which is the controlling mechanism until time t_C, and $k_S.a_S$ is the internal mass transfer coefficient, which is the controlling stage during the last steps of the extraction starting from time t_{C_2}. In the intermediate range between time t_{C_1} and t_{C_2} both mechanisms are significant, and the factor F characterizes if this intermediate stage is controlling of the global extraction process: with F=0, this stage is not significant, while with F=1 this intermediate stage in which internal and external diffusion steps are controlling mechanisms is the predominant stage during the extraction.

https://doi.org/10.1016/j.supflu.2020.105046

$$K.a = \frac{k_{SCF}.a_{SCF}.\left(\frac{F}{1+e^{-(t-t_{c_1})}}\right)}{1+e^{(t-t_{c_2})}} + \frac{k_S.a_S}{1+e^{(t-t_{c_2})}} \quad (1)$$

The mass transfer coefficient was correlated to the experimental extraction curve by minimization the Absolute Average Deviation (A.A.D.) between experimental and calculated results, defined in eq. (2). Furthermore, the correlation coefficient R^2 was calculated as defined in eq. (3) to better characterize the agreement between experiments and calculations.

$$A.A.D. = \sum_{i=1}^{n} \frac{1}{n} \frac{|x_{iEXP} - x_{iSIM}|}{x_{iEXP}}.100 \quad (2)$$

$$R^2 = \frac{\sum(x-\overline{x})(y-\bar{y})}{\sum(x-\overline{x})^2 \sum(y-\overline{y})^2} \quad (3)$$

3. Results and discussion

3.1 Supercritical fluid extraction experiments

Table 2 presents the extraction experiments performed together with the main results obtained regarding the total extraction yield and the concentration of solanesol and nicotine in the extract. As key process parameters, three CO_2 densities were considered: 781 kg/m^3, 882 kg/m^3 and 940 kg/m^3. The amount of raw material used in the experiment was either 300 g or 600 g. In addition, the influence of the compaction of the bed was also analyzed: in some experiments the bed was compacted by hand pressing, while in others a bed with its spontaneous porosity without compaction was considered. In both cases the final volume of the bed was measured afterwards. The experiments 1 and 2 was performed by duplicate to check the reproducibility, table 3 presents the average absolute deviation of these experiments.

https://doi.org/10.1016/j.supflu.2020.105046

Table 2. Supercritical fluid extraction experiments and experimental results

Exp.	RM (g)	Density CO_2 (kg/m^3)	P (MPa)	T (°C)	Bed compaction	Flowrate CO_2 (kg/h)	Mass CO_2 (kg)	Yield (g/kg RM)	Solanesol Yield (g/kg RM)	Nicotine Yield (g/kg RM)	Solanesol/ Nicotine ratio
1[a]	600	882	37	58	Yes	10.26	30.77	99.37	26.33	1.88	14.00
1[b]	600	882	37	58	Yes	10.63	31.90	86.34	22.01	1.90	11.58
2[a]	600	781	15	40	Yes	16.38	49.13	64.17	17.05	0.96	17.76
2[b]	600	781	15	40	Yes	14.33	43.00	53.60	16.13	0.97	16.63
3	600	882	37	58	No	6.83	20.50	82.30	26.74	s.d.	s.d.
4	600	781	15	40	No	15.67	47.00	50.90	33.33	s.d	s.d
5	300	882	37	58	Yes	11.67	35.00	60.02	17.52	2.10	8.34
6	300	781	15	40	Yes	16.50	49.50	46.98	16.72	1.36	12.29
7	300	882	37	58	No	7.83	23.50	43.50	11.44	1.52	7.52
8	300	781	15	40	No	18.6	45.80	34.53	4.69	0.79	5.94
9	600	940	37	40	Yes	8.57	25.70	72.51	20.08	1.23	16.32

RM: Raw Material. s.d.: no data. In exp 3 and 4 nicotine content could not be measured

Table 3. Absolute Average Deviation (A.A.D.) of experiments 1 and 2 performed in duplicate

Exp.	1[a]	1[b]	2[a]	2[b]
A.A.D.	2,49 %	4,39 %	1,81 %	8,75 %

As presented in Table 2, extraction yields increase in all cases when the bed is compacted. This result may be due to a higher porosity in the beds without compaction, which produces a worse contact between solid and CO_2 with possible formation of preferential paths. Moreover, the yields drastically decrease when the amount of raw material used is reduced to 300 g. With this lower amount, a significant space of the extractor vessel remains empty and the generation of shortcut paths can be further promoted. On the other hand, it is observed that the extraction yield increases when pressure or temperature is increased. In particular, temperature appears as a significant parameter determining the extraction yield, while density, that combines the influence of temperature and pressure, does not have a clear influence as a standalone parameter, because experiment 9, with a density of 940 kg/m^3, produced lower yields than experiment 1, carried out at a lower density of 882 kg/m^3 but a higher temperature of 58 °C. This observation can be further explained considering the results presented in Figure 2, which compares the extraction curves obtained at different CO_2 densities. The data of experiments 1 and 2 in the Figure 2 correspond to the average of experiments 1a with 1b and 2a with 2b. As presented in this Figure, the extraction curves obtained in experiments 1 and 9 are very similar,

https://doi.org/10.1016/j.supflu.2020.105046

with equal slopes in the initial linear stage of the extraction curve that indicate an equivalent solubility with these combination of pressure and temperature values, while in experiment 2 lower initial slope corresponding to a smaller solubility is observed. The slope of the curve in the first stage is not perfectly linear. But it remains constant within certain limits

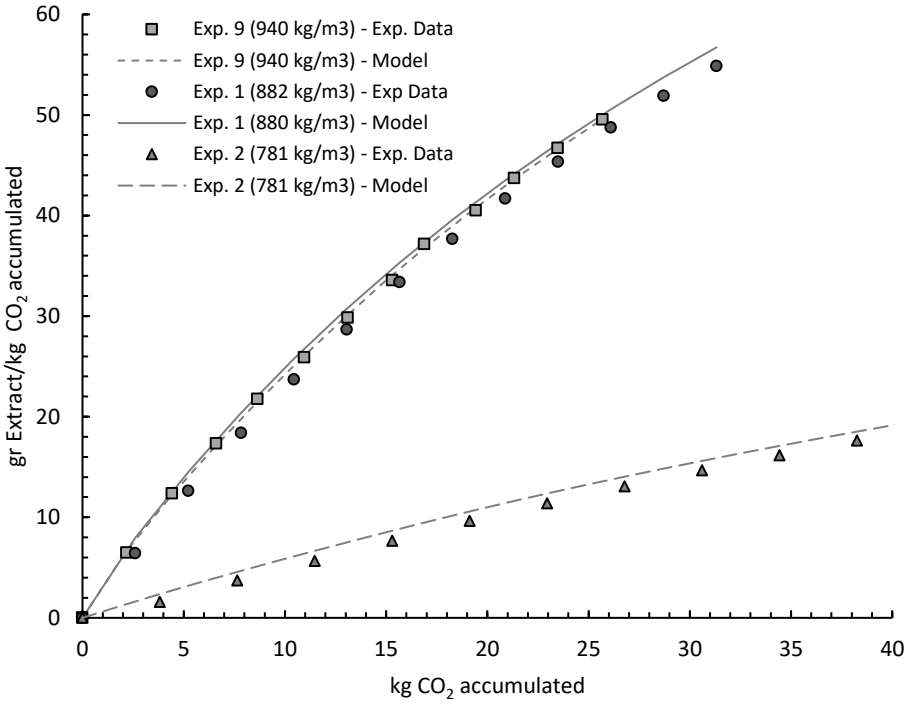

Figure 2. Extraction curves with different fluid densities

With respect to solanesol extraction, the best results were achieved with experiment 1a, which yielded 26.33 g solanesol/kg raw material operating at 37 MPa and 58 °C. Comparing with literature results, a ratio of 12.29 g solanesol/g nicotine was obtained in experiment 6 (781 kg/m3, 40 °C, 15 MPa), which is very similar to the value of 12.20 reported by Ruiz-Rodriguez et al. [20] in an extraction experiment performed at similar conditions (781 kg/m3, 40 °C, 15 MPa). With respect to the extraction of nicotine, the best results were obtained with the conditions of experiment 5 (37 MPa, 58 °C) and, finally, if the objective is the maximization of the selectivity of the extraction expressed as the ratio between the amount of solanesol extracted and the amount of nicotine extracted, the best results are obtained in experiment 2 (15 MPa, 40 °C) with a ratio of approximately 17. These results suggest that a possible strategy to obtain the highest

https://doi.org/10.1016/j.supflu.2020.105046

possible amount of solanesol and nicotine in a single extraction could be to perform a two-step extraction, with a first step carried out at 15 MPa and 40 °C and a second step carried out at 37 MPa and 58 °C. With this method, two extract fractions would be obtained, a first one with a high solanesol/nicotine ratio, and a second one with a lower amount of solanesol and a high nicotine recovery, thus facilitating the subsequent fractionation and purification of these compounds.

3.2 Phenomenological modelling

The phenomenological model of the supercritical fluid extraction developed by Cabeza et al. [25] has been used to model the extraction curves obtained. Figure 2 compares the experimental extraction curves with model results. As presented in this figure, a good correlation between experimental and model results is obtained. This observation is confirmed by the measurements of the Absolute Average Deviation (A.A.D.) between the simulated (x_{iSIM}) and experimental yield (x_{iEXP}) of the model reported in Table 4, which show high coefficients of determination (over 0.99) and small A.A.D. (below 4.70%).

Table 4: Comparison between experimental and model results

Experiment	1	2	9
A.A.D.	2.98 %	4.61 %	2.28 %
R^2	0.998	0.997	0.997

Besides the extraction curves, the model allows calculating the composition profiles along the solid and fluid phases as a function of time. Representative results are presented in Figure 3, where the simulation results corresponding to experiments 1 and 2 are presented.

https://doi.org/10.1016/j.supflu.2020.105046

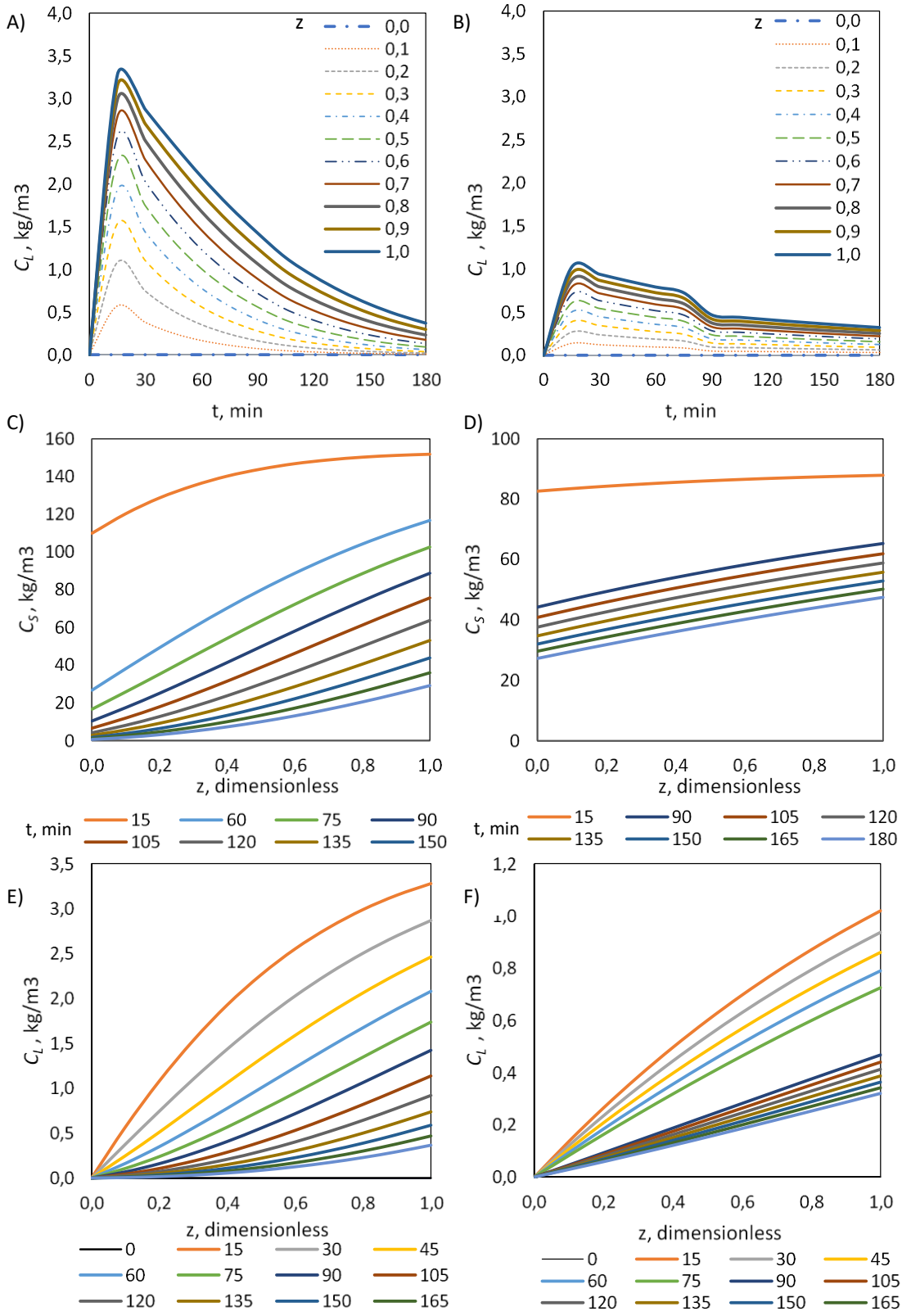

Figure 3. A) Concentration of the extract as a function of time in the supercritical phase along the extractor for experiment 1, z = 0 corresponds to the bottom and z = 1 at the top of the extractor. B) Idem to A for experiment 2. C) Concentration of the extract in the solid phase as function of z, along the time, for experiment 1. D) Idem to C, for experiment 2. E) Concentration of the extract in the supercritical phase as function of z, along the time, for experiment 1. F) Idem to E, for experiment 2.

https://doi.org/10.1016/j.supflu.2020.105046

Regarding the composition profiles in the fluid phase (Figure 3 A and B), comparing the results of experiment 1 and 2 it can be observed that while in experimental conditions 1 the concentration profiles significantly decrease along time (in correspondence to the reduction of the remaining solute amount in the solid), in experimental conditions 2 a flatter composition profile with time is observed which remains at nearly the maximum concentration value during the first 50 minutes of extraction, which suggests that in these conditions the concentration of solutes in CO_2 is close to the saturation values.

Moreover, the correlation of the model to experimental extraction curves provides an estimation of the key properties during the extraction and, in particular, of solubility and mass transfer coefficients [24]. In principle, solubility is expected to depend on fluid density, increasing at higher fluid densities, as well as on temperature due to the effect of temperature on sublimation pressure. Experimental solubilities are reported on Table 4. These solubilities were calculated as the ratio between the amount of extract recovered in the separator after 15 min of extraction and the CO_2 mass. On the other hand, Table 5 also reports the solubilities estimated with the mathematical model, which as the experimental solubilities were calculated as the ratio between the amount of extract predicted by the model after 15 min if extraction and CO_2 mass. It can be observed that experimental and estimated solubilities show a good agreement. Moreover, as presented in Figure 2, similar results regarding solubility were obtained in experiments 1 and 9, while the results of experiment 2 indicated a lower value of solubility under these conditions. Table 5 also reports the partition coefficient *h*, defined as the ratio between the concentration of the extract in the solid C_S and the concentration in the fluid C_L at time t (15 min), while V_S and V_L are the volumes of the solid and the fluid phases, respectively, at this time.

https://doi.org/10.1016/j.supflu.2020.105046

Table 4. Estimated experimental solubilities of extract

Exp.	Density CO_2 (kg/m³)	P (MPa)	T (°C)	t (min)	Extract (kg)	CO_2 (kg)	$S_{experimental}$ (kg Ext/kg CO_2)
1	882	37	58	15	0,0100	3,02	0,0033
2	781	15	40	15	0,0097	9,50	0,0010
9	940	37	40	15	0,0197	6,60	0,0030

Table 5. Solubility of extract calculated with model results

Exp.	T (min)	Q_{CO2} (g/min)	CO_2 (kg)	h (adim)	C_s (kg/m³)	V_S (m³)	C_L (kg/m³)	V_L (m³)	S_{model} (kg Ext/kg CO_2)
1	15	174	2,61	0,0240	151,77	0,00034	3,6425	0,00228	0,0032
2	15	255	3,83	0,0205	87,96	0,00064	1,8032	0,00213	0,0010
9	15	142	2,13	0,0260	108,81	0,00050	2,8291	0,00212	0,0028

Table 6. Estimated mass transfer coefficients

Exp.	R.M. (kg)	Density CO_2 (kg/m³)	P. (MPa)	T. (°C)	$k_{SCF}.a_{SCF}$ (min^{-1})	$k_S.a_S$ (min^{-1})	t_{C_1} (min)	t_{C_2} (min)	F (adim.)	R^2	A.A.D. (%)
1[a]	0.6	882	37	58	0.170	0.160	60	90	1.00	9.98E-01	2.98
2[a]	0.6	781	15	40	0.099	0.060	50	80	1.00	9.97E-01	4.61
3	0.6	882	37	58	0.110	0.048	35	55	1.00	9.95E-01	2.28
4	0.6	781	15	40	0.298	0.055	20	100	1.00	9.98E-01	2.75
5	0.3	882	37	58	0.076	0.020	50	80	1.00	9.99E-01	2.23
6	0.3	781	15	40	0.129	0.045	30	90	1.00	9.98E-01	2.82
7	0.3	882	37	58	0.300	0.045	60	90	0.50	9.97E-01	3.50
8	0.3	781	15	40	0.079	0.032	15	55	1.00	9.95E-01	3.89
9	0.6	940	37	40	0.160	0.070	50	105	1.00	9.97E-01	2.28

On the other hand, Table 6 reports the estimated mass transfer coefficients. The experiments with a highest yield in the first extraction stage, which is controlled by solubility, show a shorter t_{c1} time, as it is the case of experiments 1 and 3. Experiments that produced a lower yield, such as experiment 7, show a lower h value and a higher internal mass transfer coefficient than experiments with higher yield.

3.3 Liquid-Liquid fractionation experiments

As previously described, the objective of liquid-liquid extraction experiments was the separation of nicotine and solanesol obtained in extracts. As a first result, it must be mentioned that the

https://doi.org/10.1016/j.supflu.2020.105046

formation of a gelatinous interface was observed between the organic and the aqueous phase, in which a certain amount of extracts could be present and lost since this fraction could not be recovered and analyzed.

In HPLC analyses of the petroleum ether phase nicotine is not detected. Therefore it can be concluded that nicotine is completely eliminated from this phase down to a concentration below the detection limit. On the other hand, solanesol is distributed between the two phases: in the first stage of the separation, 55 % of solanesol remains in the ethanol-water phase and 36 % in the petroleum ether phase . This result is consistent with the results presented by Liu et al. [28] who demonstrated that solanesol is highly soluble in ethanol but has a low solubility in ether.

As previously described, after vacuum evaporation the nicotine and solanesol mixture obtained after solvent removal from the ethanol-water phase was extracted with water at pH 10 in order to extract nicotine, and the remaining solanesol after nicotine extraction was combined with the ether extract. After this process, two fractions were obtained: the ether fraction, that contained 91 % of the initial solanesol amount in the CO2 extract and whose nicotine content was below the detection limit, and the ethanol-water phase that contained 75 % of the initial nicotine amount.

Conclusions

The supercritical CO2 extraction of solanesol and nicotine from tobacco scrap residues has been researched. Pressure is a key process parameter which determines extraction yield and selectivity, because the highest extraction yield of solanesol (33.33 g solanesol/kg raw material) was achieved at an operating pressure of 15 MPa, while the highest extraction yield of nicotine (2.10 g solanesol/kg raw material) was obtained at a higher operating pressure of 37 MPa. This suggests the convenience of carrying out a two-stage extraction process in which most solanesol is extracted in a first step at low pressure, while nicotine is recovered in a second step at a higher pressure. Also, these results suggest that a possible strategy of operation to maximize the

https://doi.org/10.1016/j.supflu.2020.105046

amount of solanesol and nicotine in a single extraction, can be carried out in 2 steps. The first step to 15 MPa and 40 °C and the second to 37 MPa and 58 °C. This strategy would be valid for the configuration of the equipment used in this work, of an extractor and a separator. Modeling results indicate that the best results are achieved at conditions in which the extraction is limited by solubility. After a liquid-liquid fractionation process, two product streams were obtained: an ether fraction containing 91% of the extracted solanesol and an alcoholic fraction containing 75% of nicotine. These results demonstrate the feasibility of using tobacco waste fractions such as tobacco scrap as sources of valuable compounds and as a means of valorization of these residual fractions.

Acknowledgements

The authors thank the Spanish Ministry of Economy and Competitiveness and European Commission (FEDER) for funding the Project CTQ201679777-R. G. J. T. thanks to Santander Bank Iberoamerica Scholarships for Young Professors and Researchers progam, Eramus Mundus AMIDILA program, the Salta Tobacco Producers Cooperative for providing the tobacco and Catholic University of Salta for funding the project 196/18.

https://doi.org/10.1016/j.supflu.2020.105046

References

[1] 2019 FAO, FAOSTAT. (2017). http://www.fao.org/faostat/en/#data/QC (accessed March 2020).
[2] Ministerio de Agricultura de la Nación Argentina, Mercado interno, (2018). https://www.agroindustria.gob.ar/sitio/areas/tabaco/produccion_mercados/interno/index.php (accessed March 2020).
[3] J.C. Leffingwell, Nitrogen components of leaf and their relationship to smoking quality and aroma, Recent Adv. Tob. Sci. 2 (1976) 1-31.
[4] C. Ministerio de Hacienda y Finanzas públicas de la nación Argentina, Tabaco, 1. 32 (2016). https://www.economia.gob.ar/peconomica/docs/SSPE_Cadenas%20de%20valor_Tabaco.pdf (accessed March 2020).
[5] T. Pang, C. Bai, Y. Xu, P.D.G. Xu, Z. Yuan, Y. Su, L. Peng, Determination of Sugars in Tobacco Leaf by HPLC with Evaporative Light Scattering Detection, J. Liq. Chromatogr. Relat. Technol. 29 (2006) 1281–1289. doi:10.1080/10826070600598993.
[6] T. Rosales-Garcia, C. Jimenez-Martinez, G. Davila-Ortiz, Squalene Extraction: Biological Sources and Extraction Methods, Int. J. Environ. Agric. Biotechnol. 2 (2017) 1662–1670. doi:10.22161/ijeab/2.4.26.
[7] P. Fantozzi, A. Sensidoni, Protein extraction from tobacco leaves: technological, nutritional and agronomical aspects, Plant Foods Hum. Nutr. 32 (1983) 351–368. doi:10.1007/BF01091194.
[8] W. Huang, Z. Li, H. Niu, J. Wang, Y. Qin, Bioactivity of solanesol extracted from tobacco leaves with carbon dioxide–ethanol fluids, Biochem. Eng. J. 42 (2008) 92–96. doi:10.1016/j.bej.2008.06.002.
[9] M. Fischer, T.M. Jefferies, Optimization of Nicotine Extraction from Tobacco Using Supercritical Fluid Technology with Dynamic Extraction Modeling, J. Agric. Food Chem. 44 (1996) 1258–1264. doi:10.1021/jf950502+.
[10] N. Yan, Y. Liu, D. Gong, Y. Du, H. Zhang, Z. Zhang, Solanesol: a review of its resources, derivatives, bioactivities, medicinal applications, and biosynthesis, Phytochem. Rev. (2015) 1–15. doi:10.1007/s11101-015-9393-5.
[11] C. Zhao, Y. Zu, C. Li, C. Tian, Distribution of solanesol in Nicotiana tabacum, J. For. Res. 18 (2007) 69–72. doi:10.1007/s11676-007-0013-0.
[12] S.R. Atla, B. Raja, B.R. Dontamsetti, A new method of synthesis of coenzyme Q10 from isolated solanesol from tobacco waste, Int. J. Pharm. Pharm. Sci. 6 (2014) 499–502.
[13] K. Hamamura, I. Yamatsu, N. Minami, Y. Yamagishi, Y. Inai, S. Kijima, T. Nakamura, Synthesis of [3'-14C] coenzyme Q10, J. Label. Compd. Radiopharm. 45 (2002) 823–829. doi:10.1002/jlcr.588.
[14] Y. Naruta, Regio- and stereoselective synthesis of coenzymes Qn (n = 2-10), vitamin K, and related polyprenylquinones, J. Org. Chem. 45 (1980) 4097–4104. doi:10.1021/jo01309a006.
[15] H.-S. Wu, J.-J. Tsai, Separation and purification of coenzyme Q10 from Rhodobacter sphaeroides, J. Taiwan Inst. Chem. Eng. 44 (2013) 872–878. doi:10.1016/j.jtice.2013.03.013.
[16] Y. Tian, T. Yue, Y. Yuan, P.K. Soma, P.D. Williams, P.A. Machado, H. Fu, R.J. Kratochvil, C. Wei, Y.M. Lo, Tobacco biomass hydrolysate enhances coenzyme Q10 production using photosynthetic Rhodospirillum rubrum, Bioresour. Technol. 101 (2010) 7877–7881. doi:10.1016/j.biortech.2010.05.020.
[17] L. Qiu, H. Ding, W. Wang, Z. Kong, X. Li, Y. Shi, W. Zhong, Coenzyme Q10 production by immobilized Sphingomonas sp. ZUTE03 via a conversion–extraction coupled process in a three-phase fluidized bed reactor, Enzyme Microb. Technol. 50 (2012) 137–142. doi:10.1016/j.enzmictec.2011.11.006.
[18] M.A. Taylor, P.D. Fraser, Solanesol: Added value from Solanaceous waste, Phytochemistry. 72 (2011) 1323–1327. doi:10.1016/j.phytochem.2011.03.015.

https://doi.org/10.1016/j.supflu.2020.105046

[19] P.A. Machado, H. Fu, R.J. Kratochvil, Y. Yuan, T.-S. Hahm, C.M. Sabliov, C. Wei, Y.M. Lo, Recovery of solanesol from tobacco as a value-added byproduct for alternative applications, Bioresour. Technol. 101 (2010) 1091–1096. doi:10.1016/j.biortech.2009.09.009.
[20] A. Ruiz-Rodriguez, M.-R. Bronze, M.N. da Ponte, Supercritical fluid extraction of tobacco leaves: A preliminary study on the extraction of solanesol, J. Supercrit. Fluids. 45 (2008) 171–176. doi:10.1016/j.supflu.2007.10.011.
[21] Y. Wang, W. Gu, Study on supercritical fluid extraction of solanesol from industrial tobacco waste, J. Supercrit. Fluids. 138 (2018) 228–237. doi:10.1016/j.supflu.2018.05.001.
[22] J. Rincón, A.D. Lucas, M.A. García, A. García, A. Alvarez, A. Carnicer, Preliminary Study on the Supercritical Carbon Dioxide Extraction of Nicotine from Tobacco Wastes, Sep. Sci. Technol. 33 (1998) 411–423. doi:10.1080/01496399808544776.
[23] R.-S. Hu, J. Wang, H. Li, H. Ni, Y.-F. Chen, Y.-W. Zhang, S.-P. Xiang, H.-H. Li, Simultaneous extraction of nicotine and solanesol from waste tobacco materials by the column chromatographic extraction method and their separation and purification, Sep. Purif. Technol. 146 (2015) 1–7. doi:10.1016/j.seppur.2015.03.016.
[24] A. Cabeza, F. Sobrón, J. García-Serna, M.J. Cocero, Simulation of the supercritical CO2 extraction from natural matrices in packed bed columns: User-friendly simulator tool using Excel, J. Supercrit. Fluids. 116 (2016) 198–208. doi:10.1016/j.supflu.2016.05.020.
[25] H. Sovová, Rate of the vegetable oil extraction with supercritical CO2—I. Modelling of extraction curves, Chem. Eng. Sci. 49 (1994) 409–414
[26] P. A. Newhouse, A. Potter, M. Kelton, y J. Corwin, «Nicotinic treatment of Alzheimer's disease», Biological Psychiatry, vol. 49, n.o 3, pp. 268-278, feb. 2001, doi: 10.1016/S0006-3223(00)01069-6.
[27] M. C. Kelton, H. J. Kahn, C. L. Conrath, y P. A. Newhouse, «The effects of nicotine on Parkinson's disease», Brain Cogn, vol. 43, n.o 1-3, pp. 274-282, ago. 2000.
[28] J.-C. Liu, D.-Q. Li, R.-Q. Zhou, y F. Hao, «Solubilities of solanesol in acetonitrile, ethanol and n-hexane from 285 to 310K», Korean J. Chem. Eng., vol. 24, n.o 1, pp. 113-115, ene. 2007.